

## Thermal Expansion of Single-Crystal H<sub>2</sub>O and D<sub>2</sub>O Ice Ih

David T. W. Buckingham,<sup>1</sup> J. J. Neumeier,<sup>1,\*</sup> Sueli H. Masunaga,<sup>1,†</sup> and Yi-Kuo Yu<sup>2</sup>

<sup>1</sup>*Physics Department, Montana State University, Bozeman, Montana 59717-3840, USA*

<sup>2</sup>*National Center for Biotechnology Information, 8600 Rockville Pike, Bethesda, Maryland 20894, USA*

 (Received 20 May 2018; revised manuscript received 6 October 2018; published 2 November 2018)

Thermal expansion of H<sub>2</sub>O and D<sub>2</sub>O ice Ih with relative resolution of 1 ppb is reported. A large transition in the thermal expansion coefficient at 101 K in H<sub>2</sub>O moves to 125 K in D<sub>2</sub>O, revealing one of the largest-known isotope effects. Rotational oscillatory modes that couple poorly to phonons, i.e., lattice solitons, may be responsible.

DOI: [10.1103/PhysRevLett.121.185505](https://doi.org/10.1103/PhysRevLett.121.185505)

The form of ice most familiar to man is known as ordinary ice. It has a hexagonal-close-packed (hcp) crystal structure commonly referred to as ice Ih, where the H<sub>2</sub>O molecules remain intact with the oxygens fixed on the hcp lattice sites [1,2]. The hydrogens assume one of two possible positions between neighboring oxygens. They are 1 Å from an oxygen when they belong to a H<sub>2</sub>O molecule or 1.75 Å away when they provide the hydrogen bond to a neighboring molecule, effectively forming a double-well potential for the hydrogen between neighboring oxygens [3]. Six possible orientations of each H<sub>2</sub>O molecule exist within the hcp structure [1,2,4]. The orientations of the molecules are random, resulting in disorder of the hydrogens. Dispersion of the hydrogen positions along hydrogen bonds [2] also exists. Furthermore, the hexagonal lattice requires a bond angle between the oxygens of 109.5°; however, 104.5° is the H-O-H angle for the H<sub>2</sub>O molecule in the vapor phase [5]. The observed H-O-H angle in ice Ih lies between these two values [6], which also leads to disorder. These sources of disorder and the double-well potential result in an anharmonic energy landscape for each atom of ordinary ice.

Anharmonic atomic vibrations are responsible for the thermal expansion of solids [7,8]. Although the thermal expansion of ordinary ice has been previously measured [7,9–12], the measurements presented here utilize capacitive dilatometry, which can resolve length changes of 0.1 Å [13–15]. The relative resolution is about 1 ppb for the single crystals measured herein, which is 4000 times higher than past dilatometry measurements [10] and 8000–30 000 times higher than lattice parameter measurements [11,12]. The data reveal features in the thermal expansion of ice Ih that have not previously been observed. This includes an extremely large transition in the thermal expansion coefficient at 101 K, corresponding to the temperature where the frozen-in electric polarization is released. When ice made from D<sub>2</sub>O is measured, the transition moves to 125 K, revealing one of the largest-known isotope effects [21–23]. The shift in the transition temperature is calculated within

1% using a lattice-soliton model involving molecular rotations.

The change in sample length  $\Delta L$  normalized to the length at 10 K,  $L_{10\text{ K}}$ , of H<sub>2</sub>O and D<sub>2</sub>O ice Ih is shown in Figs. 1(a) and 2(a) for the  $a$  and  $c$  crystallographic directions. The  $\Delta L/L_{10\text{ K}}$  data span the temperature range  $5 < T < 265$  K with over 1300 individual data points. These are raw data, with no postprocessing beyond corrections for an addenda and the thermal expansion of fused silica (see Supplemental Material [15]). H<sub>2</sub>O ice [Fig. 1(a)] displays subtle anisotropy between  $a$  and  $c$ . A kink is evident at 101 K along  $c$ . Distinct minima in  $\Delta L/L_{10\text{ K}}$  are visible in the inset of Fig. 1(a) along both  $a$  and  $c$  near 63 K. The kink near 101 K and the minimum near 63 K were also observed in measurements by the authors on polycrystalline ice. The data for D<sub>2</sub>O ice [Fig. 2(a)] are similar, although the kink is near 125 K.

Differentiating  $\Delta L/L_{10\text{ K}}$  yields the thermal expansion coefficient  $\alpha = d(\Delta L/L_{10\text{ K}})/dT$  [see Figs. 1(b) and 2(b)]. Note that  $\alpha \rightarrow 0$  as  $T \rightarrow 0$  K for H<sub>2</sub>O and D<sub>2</sub>O, in agreement with the third law of thermodynamics. Focusing on H<sub>2</sub>O [Fig. 1(b)], a large feature is evident in the  $c$ -axis data, which was not resolved in prior experiments [9–12]. Its relative magnitude  $\Delta\alpha/\alpha = +220\%$ , is 100 times larger than the corresponding feature in the specific heat [24], and it is 26% of the overall change in  $\alpha$  along  $c$  for  $5 < T < 265$  K. It is  $\sim 11$  K wide (neglecting the step between 85 and 95 K) with its midpoint at 101 K. It is hereafter referred to as the “glass temperature”  $T_g$ . There is a more subtle feature along  $a$  between 104 and 128 K, noticeable as a small decrease in the slope of  $\alpha$ . There is a second, much weaker increase and then decrease in the slope of  $\alpha$  starting at 165 K, ending at 212 K, that is most pronounced along  $a$ , but also visible along  $c$  in the same temperature interval. The  $\alpha$  data for D<sub>2</sub>O along  $c$  reveal that  $T_g$  moves up considerably with its midpoint at 125 K, transition width of 13 K, broad step between 111 and 118 K, and  $\Delta\alpha/\alpha = +64\%$ . Along  $a$ , the feature occurs between 112 and 138 K, noticeable as a small decrease in the slope of  $\alpha$ . There is a second, much weaker decrease in the

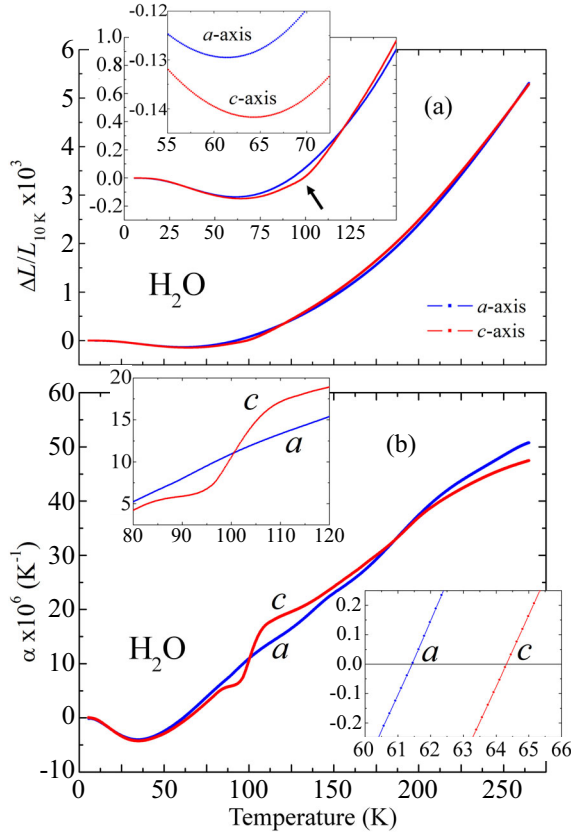


FIG. 1. (a) Linear thermal expansion  $\Delta L/L_{10\text{K}}$  of single-crystalline  $\text{H}_2\text{O}$  ice Ih along the  $a$  and  $c$  axes. (b) Thermal expansion coefficient  $\alpha$ . (Insets) Additional detail of the regions near  $T_g$  (note arrow) and where  $\alpha$  becomes negative.

slope near 178 K that seems to conclude near 214 K, visible only along  $a$ .

The temperature below which the negative thermal expansion (NE) occurs ( $\alpha < 0$ ) is defined as  $T_{\text{NE}2}$  (lower insets of Figs. 1 and 2). Below  $T_{\text{NE}2}$  the sample expands upon cooling. For  $\text{H}_2\text{O}$ ,  $T_{\text{NE}2} = 61.3(1)$  K along  $a$  and  $64.3(1)$  K along  $c$ . For  $\text{D}_2\text{O}$ ,  $T_{\text{NE}2} = 60.5(1)$  K along  $a$  and  $62.9(1)$  K along  $c$ , shifts of 0.8 and 1.4 K for  $a$  and  $c$ , respectively, that are associated with the more massive deuterium atom. The temperatures corresponding to the minima of  $\alpha$  ( $T_{\text{NE}1}$ ) along  $a$  are  $35.8(1)$  and  $35.7(1)$  K and along  $c$  are  $36.0(1)$  and  $36.5(1)$  K for  $\text{H}_2\text{O}$  and  $\text{D}_2\text{O}$ , respectively, do not change appreciably. Prior measurements could not accurately determine  $T_{\text{NE}1}$  and  $T_{\text{NE}2}$  [9–12].

The thermal expansion data for  $\text{H}_2\text{O}$  and  $\text{D}_2\text{O}$  are compared in Fig. 3. The similarity in the behavior and the shift in  $T_g$  are evident. Notable is that above  $T_g$   $\alpha$  is larger for  $\text{D}_2\text{O}$ . The same is true for  $\beta$ , the volume coefficient of thermal expansion, and the relative volume change  $\Delta V/V_{10\text{K}}$  [see Figs. 3(c) and 3(d)]. Prior measurements failed to reveal significant differences between  $\text{H}_2\text{O}$  and  $\text{D}_2\text{O}$  [10], but did reveal an enhancement of  $\alpha$  for  $\text{D}_2\text{O}$  above  $\sim 140$  K [11,12,25]. The specific heat in  $\text{D}_2\text{O}$  also exhibits an enhancement [26].

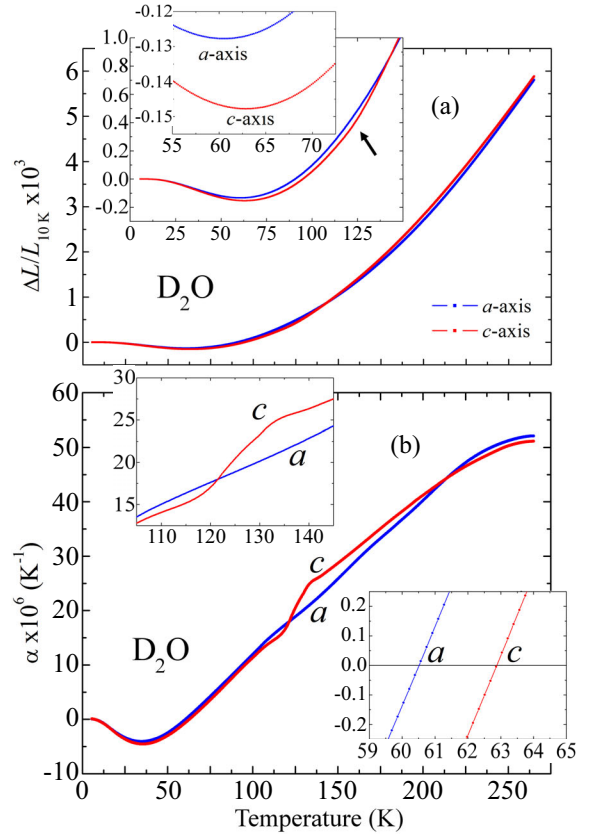


FIG. 2. (a) Linear thermal expansion  $\Delta L/L_{10\text{K}}$  of single-crystalline  $\text{D}_2\text{O}$  ice Ih along the  $a$  and  $c$  axes. (b) Thermal expansion coefficient  $\alpha$ . (Insets) Additional detail of the regions near  $T_g$  (note arrow) and where  $\alpha$  becomes negative.

The inset of Fig. 3(d) shows  $\Delta V/V_{273\text{K}}$  of  $\text{H}_2\text{O}$  liquid [27] and  $\Delta V/V_{10\text{K}}$  of  $\text{H}_2\text{O}$  ice near their minima. Ice's minimum spans a broader range in  $T$  and is about 3 times larger than the minimum in water. The  $\sim 4\%$  volume change could have implications in astrophysics;  $1\text{ m}^3$  of ice

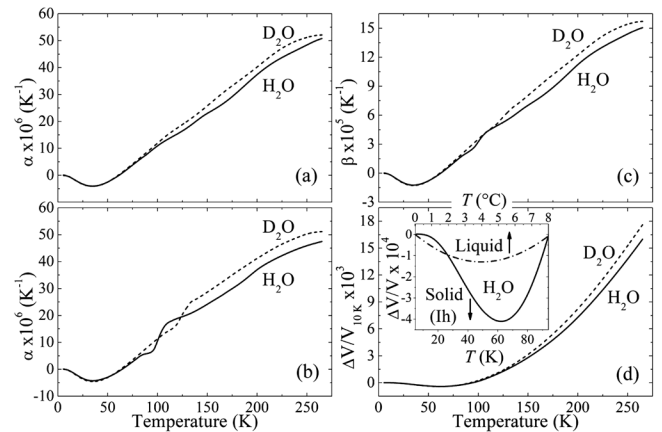


FIG. 3. (a) and (b) Comparison of the thermal expansion coefficients, (c) volumetric thermal expansion coefficients  $\beta$ , and (d) volumetric thermal expansion  $\Delta V/V_{10\text{K}}$  for  $\text{H}_2\text{O}$  and  $\text{D}_2\text{O}$  ice. (Inset) Volume minima for solid and liquid  $\text{H}_2\text{O}$ .

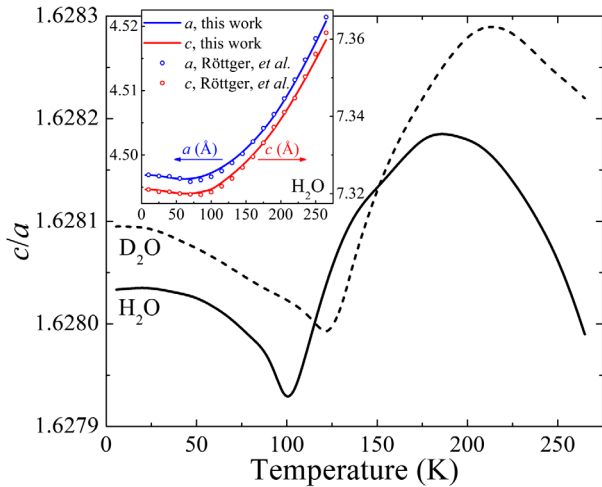


FIG. 4. The  $c/a$  ratio versus  $T$  for  $\text{H}_2\text{O}$  and  $\text{D}_2\text{O}$ . (Inset) Lattice parameters versus  $T$  for  $\text{H}_2\text{O}$  from Ref. [11] and calculated from  $\Delta L/L_{10\text{K}}$ .

embedded in a comet would exert  $\sim 4000$  Earth atmospheres of pressure [28] as it warms and cools through the minimum, leading to fragmentation.

The temperature-dependent lattice parameters are obtained after multiplying  $\Delta L/L_{10\text{K}}$  by the respective lattice parameter at 10 K [11] and adding it to that lattice parameter. The resulting  $a$  and  $c$  lattice parameters versus  $T$  for  $\text{H}_2\text{O}$  are shown in the inset of Fig. 4. The  $c/a$  ratios (main panel of Fig. 4) reveal behavior that was not observable in prior experiments. If  $c/a$  determined from lattice parameter data [11,12] were plotted in Fig. 4, the data would exhibit scatter beyond the plot's vertical boundaries. Distinct minima in  $c/a$  occur precisely at  $T_g$ , reflecting the anisotropy of  $\Delta L/L_{10\text{K}}$  imparted on ice due to the glass transition.

Solids with hcp crystal structures, including the elements Be, Zn, Cd, Ti, Zr, Co, and Tl, exhibit significant anisotropy in the thermal expansion between  $a$  and  $c$  [7], making the nearly isotropic expansion of ice Ih unusual. Ice is softer than most solids, with an isothermal bulk modulus ranging from 11 (at 0 K) to 8.4 GPa (at 273 K) [28]. The aforementioned hexagonal solids have bulk moduli 4.3–23 times larger, densities 1.8–11.9 times larger,  $a$  and  $c$  lattice parameters 1.3–2 times smaller, and thermal expansion coefficients 1.6–6.1 times smaller [7,8]. Ice's crystal structure possesses substantial empty volume [1] due to the large relative spacing between its molecules. The resulting softness and the anharmonicity noted above are likely responsible for the large magnitude of its thermal expansion. Solids with crystal structures possessing substantial empty volume, tetrahedrally bonded solids (Si and Ge, for example), and compounds sharing ice's wurtzite crystal structure (CdS and ZnO, for example) often exhibit NE [7,29]. Atomic vibrations perpendicular to the line connecting adjacent atoms, known as transverse acoustical phonons, can be the source of

NE [29]. They have been identified as being responsible for ice's NE [30–32]. The temperature  $T_{\text{NE}2}$  defines the temperature above which Grüneisen modes responsible for positive thermal expansion begin to dominate. Near 25 K, which is below  $T_{\text{NE}1}$ ,  $\alpha$  is shifted downward in temperature for  $\text{D}_2\text{O}$  from the values observed for  $\text{H}_2\text{O}$  by 2.0% along  $a$  and 4.0% along  $c$ .  $T_{\text{NE}2}$  is also shifted downward in  $\text{D}_2\text{O}$ , by 1.3% along  $a$  and 2.2% along  $c$ . The direction of these shifts and their modest magnitude indicate that the modes giving rise to negative and positive Grüneisen parameters for  $T < 70$  K probably involve vibrations of the entire molecule. Note that the ratio of  $T_{\text{NE}1}$  along  $c$ ,  $36.5(1)/36.0(1) = 1.014(5)$ , agrees well with the ratio of the dipole interaction energies for  $\text{D}_2\text{O}$  and  $\text{H}_2\text{O}$  [33], suggesting that  $T_{\text{NE}1}$  may signify the temperature above which the electric polarization along  $c$  weakens.

The large increase of  $\alpha$  at  $T_g$  proves the bulk nature of the transition. If it were first order, as expected for a transition from one crystallographic structure to another, a discontinuity in  $\Delta L/L_{10\text{K}}$  would be evident [34]. The measurements reveal no discontinuity, so this is unlikely. More rapid cooling of  $\text{H}_2\text{O}$  ice (instead of 0.2, 0.5, and 1 K/min) and then warming at 0.2 K/min moves  $T_g$  to higher temperature (+6 and +11 K, respectively) [14]. Since  $\alpha$  exhibits hysteresis about  $T_g$ , the transition is not continuous (i.e., second order) [34]. Furthermore, it is extremely broad and the transitions along  $a$  and  $c$  do not coincide in temperature. These considerations lead us to characterize it as a glass transition, in agreement with Haida *et al.* [24].

Phonons are not responsible for the upward shift of  $T_g$ , since measured phonon modes move downward in energy for  $\text{D}_2\text{O}$  versus  $\text{H}_2\text{O}$  [1,31,35]. However, it seems reasonable to assume that hydrogen motion is in some manner responsible for the transition at  $T_g$ . In principle, hydrogen motion in pure ice over the 0.75 Å distance from one oxygen to its neighbor is possible through direct transfer of a  $\text{H}^+$  ion. Since the energy to dissociate  $\text{H}_2\text{O}$  to form  $\text{H}^+$  and  $\text{OH}^-$  is extremely high [36], this process has a low probability. Direct transfer of a  $\text{H}^+$  ion through quantum-mechanical tunneling [37] has been reported, but recent experiments failed to observe any tunneling [38]. In a laboratory-accessible electric field  $E$ , if the protons in ice were to move via tunneling, the force would be negligible compared to the dissociation energy per meter, and proton tunneling would remain spatially random, leading to zero net electric polarization. Partial rotation of a  $\text{H}_2\text{O}$  molecule, equivalent to tilting of  $\vec{p}$ , the electric dipole moment, would lead to a net electric polarization [39]. Polarizing ice near its melting point with  $E$ , cooling to 80 K, setting  $E = 0$ , and observing the polarization loss upon warming leads to the thermally stimulated depolarization (TSD) current. It reveals [40] a release of the frozen-in electric polarization above 100 K. A reasonable assessment is that the  $\text{H}_2\text{O}$  molecules are held in slightly rotated positions below 100 K by local strain fields associated with ice's hydrogen disorder due to the dominance of potential energy



over kinetic energy. The thermal energy above 100 K is sufficient to release the molecules. TSD current was measured for the samples in this study with  $E$  along  $c$ , the direction where the transition at  $T_g$  is most evident. The peak in TSD current coincides with the transition in  $\alpha$  at  $T_g$  for  $\text{H}_2\text{O}$  and  $\text{D}_2\text{O}$  [15], indicating a common physical origin. Given the coincidence in temperature of the transitions in the  $\alpha$  and TSD data, the transition at  $T_g$  is attributed to hydrogen (deuteron) motion through release of  $\text{H}_2\text{O}$  ( $\text{D}_2\text{O}$ ) molecules from their frozen-in orientations below  $T_g$ .

We postulate that, once the hydrogens are released from their local strain fields above  $T_g$ , the strongly anharmonic potentials in which they exist lead to rotational oscillatory modes of the molecules that couple poorly to ice's phonon modes [41]. Comparison of the specific heats of  $\text{H}_2\text{O}$  ice and its heavy water variant  $\text{D}_2\text{O}$  [26,42,43] reveals that small-amplitude molecular rotation, also called libration, contributes significantly to the specific heat, particularly above 100 K. In our scenario, the molecular rotation is spread, along a chain, over a large number of  $\text{H}_2\text{O}$  molecules with small relative rotation from one molecule to the next, forming a wave front. That is, the  $\text{H}_2\text{O}$  molecules exhibit intrinsic localized modes (ILMs) of vibration [44], also referred to as "lattice solitons." Across the wave front, the H-O distance changes monotonically from 1.75 to 1.0 Å, effectively transferring one hydrogen. Our scenario combines the mechanism of libration with the formation of Bjerrum  $L$  and  $D$  defects [1,39,45,46]; however, the defect is spread across the wave front. The formation of ILMs would lead to a structural relaxation [41,44], thereby contributing to the thermal expansion. If the strained regions propagate, they may annihilate oppositely strained regions upon collision, resulting in a large-scale relaxation. The presence of ILMs in ice is consistent with the peak observed in the specific heat [24] since, when active, they add configurational entropy [44].

A modified version of a lattice-soliton model [3] for chainlike structures of  $\text{H}_2\text{O}$  molecules offers a possible type of ILM. To connect with the discussion above, the solitary wave front represents the local strained region and the moving wave front represents the propagation of strain. Note that zigzag, chainlike structures exist along  $c$  in ice Ih, but not in the basal plane [1]. The original model [3] considered a chain of  $\text{OH}^-$  ions with a proton placed between neighboring ions in a double-well potential with one minimum representing covalent bonding to one ion and the other representing hydrogen bonding to the same ion. In our modified version, we view a hydrogen hopping from one minimum to the next as a cooperative motion between neighboring water molecules along the chain via multiple small-amplitude molecular rotations. This allows for a continuum description in contrast to the fully discrete case of the Bjerrum rotation of one molecule at a time. For simplicity, the bond-length difference between O-H and O-D are ignored and the elastic energy

constants associated with (a) relative displacement between two neighboring oxygens and (b) relative displacement between neighboring in-line hydrogens are assumed to be identical. With these simplifications, and the assumption of weak coupling between hydrogen and oxygen motion along the chain, the result from Ref. [3] gives a relation for the energy of the lattice soliton as

$$E \propto \sqrt{\frac{\epsilon_0 M_O}{M_O - m}}, \quad (1)$$

with  $m$  as the hydrogen (deuteron) mass and  $M_O$  as the oxygen mass. Provided that the barrier height  $\epsilon_0 \propto \sqrt{m}$ , we obtain  $E_{\text{D}_2\text{O}}/E_{\text{H}_2\text{O}} \approx 1.23$ , representing the ratio of thermal energies needed for solitary wave formation in  $\text{D}_2\text{O}$  and  $\text{H}_2\text{O}$ . This is in agreement with the ratio  $T_g(\text{D}_2\text{O})/T_g(\text{H}_2\text{O}) = 1.24$ . Additional information regarding the model (1),  $\epsilon_0$ , and the  $T_g$  ratio when discrete Bjerrum rotation is used as the strain release mechanism is provided in the Supplemental Material [15].

Coincident with the large feature in  $\alpha$  along  $c$  at  $T_g$ , there is a smaller feature along  $a$ . The resulting anisotropy in  $\Delta L/L_{10\text{K}}$  is responsible for the dramatic dip in  $c/a$  at  $T_g$ . ILMs in uranium are polarized along the  $[0\ 1\ 0]$  direction [47], leading to anisotropy in its thermal expansion. If ILMs are active in ice, anisotropy in  $\alpha$  and the dip in  $c/a$  signify polarization of the ILM. Additional features in  $\alpha$  along  $a$  and  $c$ , evident in the region  $165 < T < 212$  K, may correspond to the formation of higher-order ILMs or coupling between them. Further study will be required to understand these features.

This Letter reveals new aspects regarding the thermal expansion of ice, due to the high relative resolution of the measurements. A large transition in  $\alpha$  at 101 K is shown to coincide with the release of frozen-in electric polarization and to be strongly influenced by the replacement of hydrogen with deuterium. It is attributed to the onset of lattice solitons activated by hydrogen motion along a chain of  $\text{H}_2\text{O}$  molecules via small-amplitude molecular rotation. The solitary wave front can be viewed as a screw dislocation that is restricted to the hydrogen lattice.

This research was conducted with support from the National Science Foundation under Grant No. DMR-1204146. A grant from the Office of Naval Research (N000141512775) assisted with helium liquefaction. Research at the National Center for Biotechnology Information is supported by the intramural research program of the National Institutes of Health. S. H. M. was supported by CNPq Grant No. 237050/2012-9. The authors thank Forrest Gile for technical assistance and V. H. Schmidt and D. N. Argyriou for valuable discussions. The single crystals used in this work were shaped and oriented at MSU's Subzero Research Laboratory.

\*Corresponding author.

neumeier@montana.edu

†Permanent address: Physics Department, Centro Universitário FEI, 09850-901, São Bernardo do Campo, São Paulo, Brazil.

- [1] V. F. Petrenko and R. W. Whitworth, *Physics of Ice* (Oxford University Press, New York, 1999).
- [2] W. F. Kuhs and M. S. Lehmann, in *Water Science Reviews 2: Crystalline Hydrates*, edited by F. Franks (Cambridge University Press, Cambridge, 1986), p. 1, ISBN: 9780511897504.
- [3] V. Y. Antonchenko, A. S. Davydov, and A. V. Zolotariuk, *Phys. Status Solidi B* **115**, 631 (1983).
- [4] L. Pauling, *J. Am. Chem. Soc.* **57**, 2680 (1935).
- [5] W. S. Benedict, N. Gailar, and E. K. Plyler, *J. Chem. Phys.* **24**, 1139 (1956).
- [6] V. M. Nield and R. W. Whitworth, *J. Phys. Condens. Matter* **7**, 8259 (1995).
- [7] T. H. K. Barron and G. K. White, *Heat Capacity and Thermal Expansion at Low Temperatures* (Kluwer, New York, 1999), ISBN: 0-306-46198-6.
- [8] C. Kittel, *Introduction to Solid State Physics*, 8th ed. (John Wiley & Sons, New York, 2005).
- [9] M. Jakob and S. Erk, *Wiss. Abh. Phys. Tech. Reichsanst.* **12**, 302 (1929).
- [10] G. Dantl, *Z. Phys.* **166**, 115 (1962).
- [11] K. Röttger, A. Endriss, J. Ihringer, S. Doyle, and W. F. Kuhs, *Acta Crystallogr. Sect. B* **50**, 644 (1994).
- [12] A. D. Fortes, *Acta Crystallogr. Sect. B* **74**, 196 (2018).
- [13] J. J. Neumeier, R. K. Bollinger, G. E. Timmins, C. R. Lane, R. D. Krostad, and J. Macaluso, *Rev. Sci. Instrum.* **79**, 033903 (2008).
- [14] D. T. W. Buckingham, High-resolution thermal expansion and dielectric relaxation measurements on H<sub>2</sub>O and D<sub>2</sub>O ice Ih, Ph.D. thesis, Montana State University, 2017.
- [15] See Supplemental Material at <http://link.aps.org/supplemental/10.1103/PhysRevLett.121.185505>, which includes information regarding single-crystal growth, sample preparation, measurement methods and resolution, data analysis, TSD data, and theory along with Refs. [16–20].
- [16] D. F. Shriver and M. A. Drezdson, *The Manipulation of Air-Sensitive Compounds*, 2nd ed. (Wiley, New York, 1986).
- [17] J. Bilgram, H. Wenzl, and G. Mair, *J. Cryst. Growth* **20**, 319 (1973).
- [18] C. C. Langway, Jr., Ice fabrics and the universal stage, U. S. Army Corps of Engineers: Snow, Ice, and Permafrost Research Establishment, Technical Report No. 62, 1958.
- [19] M. Okaji, N. Yamada, K. Nara, and H. Kato, *Cryogenics* **35**, 887 (1995).
- [20] J. J. Neumeier, T. Tomita, M. Debessai, J. S. Schilling, P. W. Barnes, D. G. Hinks, and J. D. Jorgensen, *Phys. Rev. B* **72**, 220505 (2005).
- [21] G.-M. Zhao, K. Conder, H. Keller, and K. A. Müller, *Nature (London)* **381**, 676 (1996).
- [22] S. Koval, J. Kohanoff, R. L. Migoni, and E. Tosatti, *Phys. Rev. Lett.* **89**, 187602 (2002).
- [23] M. Medarde, P. Lacorre, K. Conder, F. Fauth, and A. Furrer, *Phys. Rev. Lett.* **80**, 2397 (1998).
- [24] O. Haida, T. Matsuo, H. Suga, and S. Seki, *J. Chem. Thermodyn.* **6**, 815 (1974).
- [25] B. Pamuk, J. M. Soler, R. Ramírez, C. P. Herrero, P. W. Stephens, P. B. Allen, and M.-V. Fernández-Serra, *Phys. Rev. Lett.* **108**, 193003 (2012).
- [26] R. W. Blue, *J. Chem. Phys.* **22**, 280 (1954).
- [27] V. Stott and P. H. Biggs, *International Critical Tables* (McGraw-Hill, New York, 1926), Vol. 3, p. 24.
- [28] J. J. Neumeier, *J. Phys. Chem. Ref. Data* **47**, 033101 (2018).
- [29] G. D. Barrera, J. A. O. Bruno, T. H. K. Barron, and N. L. Allan, *J. Phys. Condens. Matter* **17**, R217 (2005).
- [30] H. Tanaka, *J. Mol. Liq.* **90**, 323 (2001).
- [31] S. M. Bennington, J. Li, M. J. Harris, and D. K. Ross, *Physica (Amsterdam)* **263B–264B**, 396 (1999).
- [32] T. Strässle, A. M. Saitta, S. Klotz, and M. Braden, *Phys. Rev. Lett.* **93**, 225901 (2004).
- [33] T. Matsuo, Y. Tajima, and H. Suga, *J. Phys. Chem. Solids* **47**, 165 (1986).
- [34] A. B. Pippard, *The Elements of Classical Thermodynamics* (Cambridge University Press, New York, 1957).
- [35] J.-C. Li, *J. Chem. Phys.* **105**, 6733 (1996).
- [36] O. Oldenberg, *J. Chem. Phys.* **17**, 1059 (1949).
- [37] L. E. Bove, S. Klotz, A. Paciaroni, and F. Sacchetti, *Phys. Rev. Lett.* **103**, 165901 (2009).
- [38] A. I. Kolesnikov, G. Ehlers, E. Mamontov, and A. Podlesnyak, *Phys. Rev. B* **98**, 064301 (2018).
- [39] I. Popov, I. Lunev, A. Khamzin, A. Greenbaum (Gutina), Y. Gusev, and Y. Feldman, *Phys. Chem. Chem. Phys.* **19**, 28610 (2017).
- [40] G. P. Johari and S. J. Jones, *J. Chem. Phys.* **62**, 4213 (1975).
- [41] M. E. Manley, *Acta Mater.* **58**, 2926 (2010).
- [42] A. J. Leadbetter, *Proc. R. Soc. A* **287**, 403 (1965).
- [43] P. Flubacher, A. J. Leadbetter, and J. A. Morrison, *J. Chem. Phys.* **33**, 1751 (1960).
- [44] A. J. Sievers and S. Takeno, *Phys. Rev. Lett.* **61**, 970 (1988).
- [45] N. Bjerrum, *Science* **115**, 385 (1952).
- [46] B. Geil, T. M. Kirschgen, and F. Fujara, *Phys. Rev. B* **72**, 014304 (2005).
- [47] M. E. Manley, M. Yethiraj, H. Sinn, H. M. Volz, A. Alatas, J. C. Lashley, W. L. Hults, G. H. Lander, and J. L. Smith, *Phys. Rev. Lett.* **96**, 125501 (2006).